Hindawi
Advances in Materials Science and Engineering
Volume 2022, Article ID 6806153, 10 pages
https://doi.org/10.1155/2022/6806153

Research Article

Serviceability Properties of Solid Buoyancy Materials for Deep-Sea HOV

Hailong Zhang, Guoliang Ma, and Zhiwei Zhu

Institute of Deep-Sea Science and Engineering, Chinese Academy of Sciences, Sanya 572000, China

Correspondence should be addressed to Guoliang Ma; magl2288@126.com

Received 25 August 2022; Revised 17 November 2022; Accepted 19 November 2022; Published 6 December 2022

Academic Editor: Antonio Gloria

Studying the evolution characteristics of damage strength and water absorption behavior of hollow glass beads solid buoyancy materials used for manned submersibles in the hyper-pressure environment will help people to understand the damage mechanism and induced mechanism of buoyancy materials for manned submersibles. To explore the influence mechanism of different pressure, temperature, loading rate and load cycle times on deformation, failure, and water absorption behavior of solid buoyant materials, hydrostatic pressure tests of solid buoyant materials under different conditions are conducted in this study. Based on the test data, the nonlinear characteristics of mechanical properties and water absorption behavior of two buoyant materials are obtained. The results show that the water absorption characteristics of solid buoyant materials are affected by hydrostatic pressure, and the water absorption characteristics increase exponentially as the hydrostatic pressure increases. The loading rate insignificantly affects the compressive strength and water absorption characteristics of both materials. Ambient temperature has a great influence on water absorption characteristics and failure strength of high-strength solid buoyant materials. After cyclic loading, the properties of buoyant materials decreased, and X-ray micro-CT showed that the internal hollow glass beads had a good shape and no significant change in the glass beads breakage rate. The change of solid buoyancy material properties is mainly due to the change of resin base material properties, resulting in material aging and performance attenuation. The research results are helpful to further explore the fracturing evolution and water absorption behavior of solid buoyant materials and then play a guiding role in calculating the counterweight of manned submersible operation and performance prediction and maintenance of buoyant materials for manned submersibles.

1. Introduction

Solid buoyancy material is one of the key technologies in manned submersibles. Its importance in deep-sea exploration has been widely recognized [1, 2]. The solid buoyancy material of manned submersible is composed of hollow glass beads and resin substrate by mixing and heat curing, in which hollow glass beads are the key [3, 4]. To fulfill the requirements of deep-sea exploration for China, a full deep-sea manned submersible was developed by using solid buoyancy material with domestic hollow glass beads, set a Chinese record of 10,909 meters in manned deep-sea diving in 2020, and was named "Fendouzhe." The properties of solid buoyant materials mainly include density, water absorption, and compressive strength. There are no commercial products that can provide the buoyancy material to satisfy the classification rule requirement; the decrease of compressive strength and the increase of water absorption of solid buoyancy material seriously endanger the safety and usability of the full ocean depth manned or unmanned submersibles, and thus this component should be used with specific monitoring of its damage state in order to guarantee the safety of a manned submersible operation. Therefore, studying the evolution characteristics of damage strength and water absorption behavior of solid buoyancy materials used for manned submersibles in the hyper-pressure environment will help people to understand the damage mechanism and induced mechanism of this component and then play a guiding role in calculating the counterweight of manned submersible operation and

performance prediction and maintenance of buoyant materials for manned submersibles.

Currently, studies on solid buoyancy materials mainly focus on material ratio, manufacturing process, and material strength [5–9]. The strength of the material depends on the strength and toughness of the resin matrix, the bonding strength between the matrix and microspheres, the strength of the hollow microspheres, and Poisson's ratio of components [10]. Concerning the strength of solid buoyancy materials, scholars worldwide have usually used uniaxial compression tests, high-pressure environment simulation tests, numerical simulation approaches, and other methods to determine the mechanical properties and pressure-resisting performances of buoyant materials under high-pressure environments [11–15]. Liang et al. investigated the hydrostatic pressure performance and water absorption of buoyant materials with different density characteristics and studied the relationship between the density, hydrostatic pressure, and water absorption of buoyant materials [16, 17]. Liang et al. investigated the effect of the density of a buoyant material on its water absorption characteristics under 110 MPa hydrostatic pressure [18]. Gupta and Woldesenbet investigated the micromorphology of a buoyant material after stress deformation under different local stress conditions and confirmed that there were many broken microspheres on the buoyant material's surface under compression [19]. Liang studied the fracture behavior of hollow glass beads of solid buoyancy materials [20–22]. Yan et al. studied the mechanical properties of high-performance hollow glass beads [23]. Gupta and Woldesenbet used five kinds of hollow glass beads as fillers to conduct research, and the results showed that the compression strength and compression modulus of buoyant materials increased with the increase of the strength of the beads when the epoxy resin matrix and volume filling amount were the same [24]. Kim and Plubrai carried out a study about failure mechanisms for solid buoyancy material. Two different failure modes were found, where one is characterized by longitudinal splitting and the other by layered crushing. The former occurred at a low density of foam and the latter at relatively high densities of foam, and a schematic model for the layered crushing is proposed to explain its mechanism [25]. Bo et al. studied the damage and failure behaviors of the epoxy buoyant materials after quasi-static and dynamic loadings [26]. Ozturk and Anlas carried out a study about hydrostatic compression of anisotropic low-density polymeric foams under multiple loadings [27]. Zhao et al. conducted high-pressure environmental tests to explore the damage mechanism of buoyant materials because of the damage of buoyant materials in the recent application of "Jiaolong" HOV [28]. Wang et al. proposed a theoretical model of compressive strength and water absorption of solid buoyancy materials used in full-depth submersibles [29].

In studying solid buoyancy materials for manned submersibles, the evolution law of mechanical properties and failure mechanism of solid buoyancy materials under long-term exposure to extreme deep-sea environments remain superficial and lack systematic research [30, 31]. No relevant research literature has been reported on the coupled effects of different pressure, temperature, loading rate, and load cycle times on deformation, failure, and water absorption behavior of solid buoyant materials. Currently, studies on solid buoyancy materials mainly focus on material ratio, manufacturing process, and material strength. Therefore, in this study, hydrostatic pressure tests of solid buoyant materials under different conditions were conducted and comprehensively analyzed the coupled effects of different pressure, temperature, loading rate, and load cycle times on deformation, failure, and water absorption behavior of solid buoyant materials. Secondly, the characteristics of solid buoyant materials after long-term cyclic loading were further analyzed, and the microstructure of the materials was analyzed by X-ray micro-CT. The research results are helpful to further explore the fracturing evolution and water absorption behavior of solid buoyant materials and then play a guiding role in calculating the counterweight of manned submersible operation and performance prediction and maintenance of buoyant materials for manned submersibles.

2. Experiment Overview

2.1. Experimental Materials and Equipment. The materials selected for the experiment are 4500- and 11000 m solid buoyancy materials, T-54 and T-68, independently developed by the Institute of Physical and Chemical Technology, Chinese Academy of Sciences. Figure 1 shows the buoyancy material samples for the tests, and the material parameters are shown in Table 1. The loading equipment adopts a 200 MPa controllable temperature isostatic pressure simulation test device (Figure 2). The maximum working pressure of the test device is 200 MPa, the inner diameter of the working cylinder is 180 mm, the effective height is 400 mm, the pressure-lifting speed is 0.4–25 MPa/min, the pressure value control accuracy is ±1 MPa, and the temperature control range is 2°C–35°C.

2.2. Experimental Method

2.2.1. Water Absorption Test Method. Before the experiment, the sample size was measured. Next, the sample was soaked in water for 2 min, taken out, and dried. Afterward, the sample was weighed using an electronic balance with an accuracy of 0.001 g. Furthermore, the sample was put in the controllable temperature isostatic pressure simulation test device for the hydrostatic loading test. After the hydrostatic test, the sample was taken out of the isostatic pressure test device, wiped off the water on the surface, and weighed. Next, the water absorption is calculated as follows:

$$m = \frac{m_1 - m_0}{m_0} \times 100\%, \tag{1}$$

where m_0 is the sample's mass before loading, m_1 is the sample mass after loading, and m is the water absorption of the buoyant material.

2.2.2. Measurement Method of Bulk Elastic Modulus. The bulk elastic moduli of the solid buoyancy materials were measured using an ultrasonic device (Figure 3).

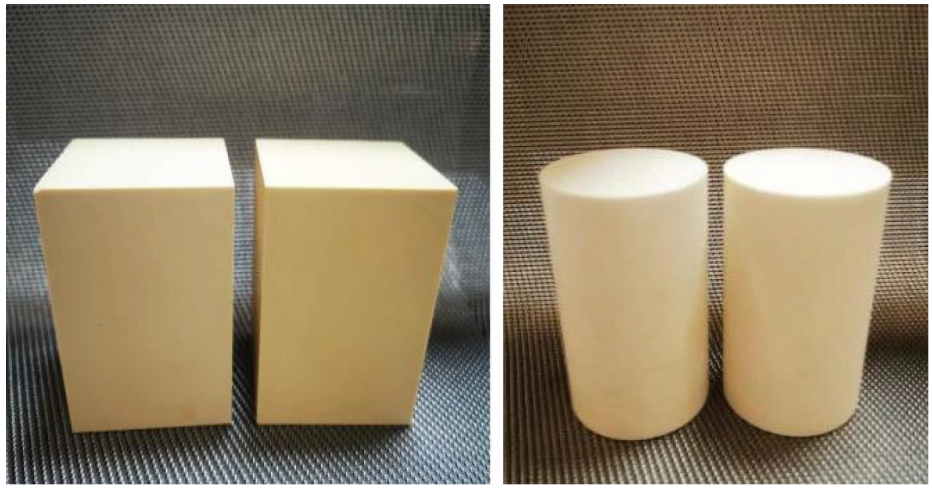

T-68 T-54

Figure 1: Two types of buoyancy materials.

Table 1: Parameters of buoyancy materials.

Type	Working depth (m)	Material density (g/cm^3)	Poisson's ratio	Size
T-54	4500	0.54	0.3	$\Phi 50 \times 100$
T-68	11000	0.68	0.3	$50 \times 50 \times 100$

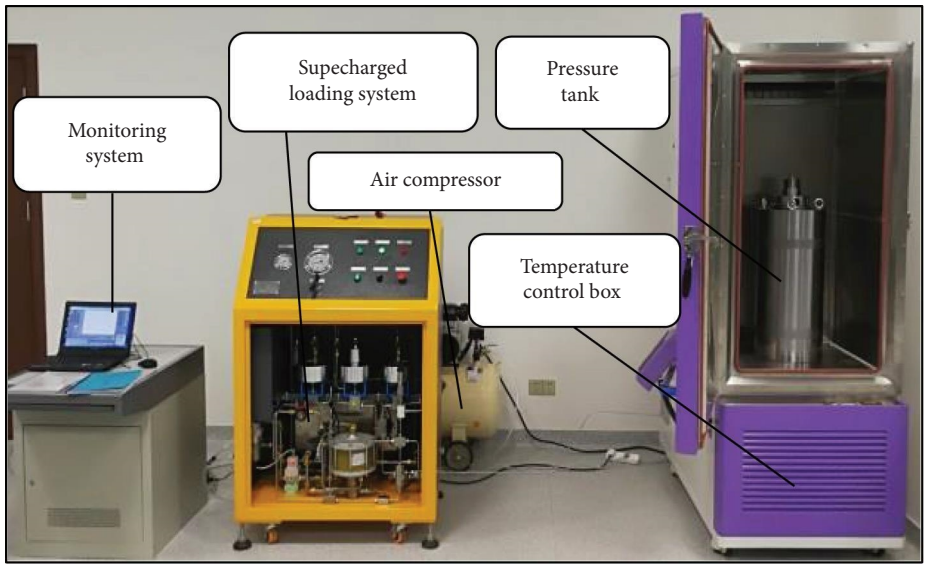

Figure 2: Controllable temperature isostatic pressure test device.

According to the ultrasonic theory, by measuring the longitudinal (C_L) and transverse (C_S) wave velocities of the solid buoyancy materials, combined with their density (ρ), the bulk elastic modulus (k) of T-54 and T-68 is calculated as follows:

$$k = \frac{\rho C_s^2 \left\{3\left(C_L/C_s\right)^2 - 4\right\}}{\left(C_L/C_s\right)^2 - 1}, \quad (2)$$

where C_L is the longitudinal wave velocities of the solid buoyancy materials, C_S is the transverse wave velocities of the solid buoyancy materials, ρ is the density of the solid buoyant materials, and k is the bulk elastic modulus of the solid buoyancy materials.

2.2.3. Test Method for the Strength of Solid Buoyancy Materials. After fixing the buoyant material, it was placed in the isostatic pressure test device. Next, the ambient temperature and loading rate were controlled. Afterward, the device was gradually pressurized to the set pressure, and the pressure holding time was calculated. After holding the pressure for the duration of the pressure

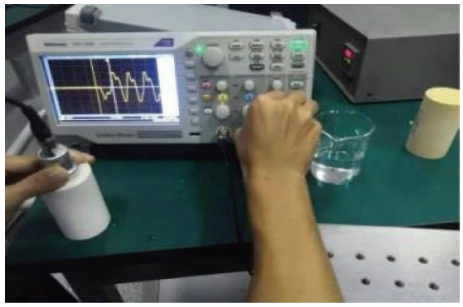

Figure 3: Acoustic measurement bulk modulus of elasticity.

holding time, the pressure is released. The loading curve in the pressure chamber during the test is shown in Figure 4.

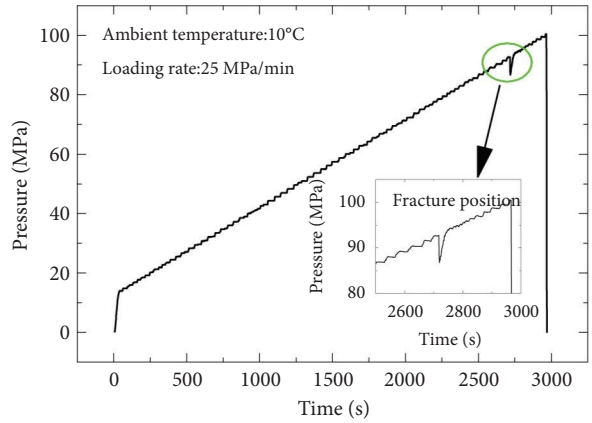

Figure 4: Ultimate strength test curve of T-54.

2.2.4. Test Scheme. The test is divided into four groups. The first group conducted the water absorption test of the material in the process of ultimate pressure failure. For two solid buoyancy materials, the water absorption and crushing strength of the material at each stage of pressure rise to failure pressure were measured. The second group loaded the material at different temperatures on the working pressure for 24 h, and the water absorption and crushing strength characteristics of the material were measured. In the third group, the materials were loaded to the working pressure at different loading rates for 0.5 h, and the water absorption and crushing strength were measured. The fourth group is the material cycle test, which measures the water absorption and crushing strength of the material under working pressure and after different cycle pressurization times. Table 2 presents the experimental parameters of each group.

3. Results and Analysis

3.1. Effect of Hydrostatic Pressure on Water Absorption. Figure 5 shows that the water absorption of the two buoyant materials increases exponentially as the hydrostatic pressure increases, and the growth trend is similar. When the hydrostatic pressure of T-54 is between 0 and 80 MPa, the increased range of water absorption is small. When the hydrostatic pressure exceeds 80 MPa, the water absorption increases exponentially until the hydrostatic pressure reaches 94 MPa and the sample is damaged. When the hydrostatic pressure of T-68 is between 0 and 100 MPa, the increase in water absorption is small. When the hydrostatic pressure exceeds 100 MPa, the water absorption increases exponentially until the sample damages after the hydrostatic pressure reaches 176 MPa. Figure 6 presents the pressure feed point area curve of *T*-68 under the ultimate strength test.

3.2. Effect of Ambient Temperature on Water Absorption and Failure Strength. The ambient temperature of the test device was controlled to 4°C, 10°C, 20°C, and 35°C, respectively, and pressurized at the rate of 2 MPa/min until the sample was pressed and fed. Next, the water absorption and strength changes of the buoyant materials under different ambient temperatures and working pressure for 24 h were investigated. Figure 7 shows that the water absorption characteristics of the two buoyant materials are incompletely affected by temperature. Between 4°C and 20°C, the water absorption characteristics of the two buoyant materials change insignificantly. Here, the water absorption characteristics of the two buoyant materials are almost the same and change between 0.1% and 0.2%. At 35°C, the water absorption of *T*-68 increases significantly to 0.33%. Furthermore, Figure 8 shows that the crushing strength of T-54 is insignificantly affected by the ambient temperature change, and the crushing strength is maintained at 94 MPa between 4°C and 35°C. Whereas the crushing strength of *T*-68 decreases as the temperature increases; the crushing strength decreases from 174 to 160 MPa. When the ambient temperature exceeds 20°C, the water absorption performance of *T*-68 increases significantly, and the crushing strength decreases. In contrast, the water absorption of T-54 is insignificantly affected by temperature change, and its crushing strength hardly changes.

3.3. Effect of Loading Rate on Water Absorption and Failure Strength. The ambient temperature of the test device was controlled to 10°C, and the sample step was pressurized at the rates of 0.6, 2, 10, 15, and 25 MPa/min, respectively, until the sample was pressure fed. Afterward, the influence of the loading rate on water absorption and crushing strength was analyzed. Figures 9 and 10 show that the water absorption characteristics of the two buoyant materials change insignificantly with the loading rate. The water absorption of T-54 increases slightly as the loading rate increases, whereas that of T-68 does not increase or decrease significantly as the loading rate increases. Comparing the influence diagram of the crushing strength of the two buoyant materials with the loading rate shows that the loading rate slightly affects the failure strength of the buoyant materials, and the crushing strength of the two materials remains unchanged as the loading rate increases.

3.4. Effect of Cyclic Loading on Water Absorption and Failure Strength. The ambient temperature of the test device was controlled to 10°C, and the device was pressurized to the

Table 2: Experimental parameters.

	Holding time	Hydrostatic pressure (MPa)	Temperature (°C)	Loading rate (MPa/min)	Number of cycles
Group 1	5 min	0–200	10	2	—
Group 2	24 h	45, 110	4, 10, 20, 35	2	—
Group 3	30 min	45, 110	10	0.6, 2, 10, 20, 25	—
Group 4	5 min	45, 110	10	25	100, 200, 400, 500, 600, 800, 1000

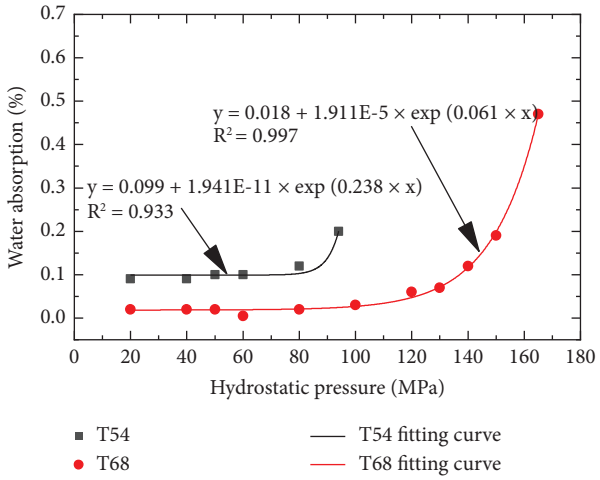

Figure 5: Water absorption vs. hydrostatic pressure.

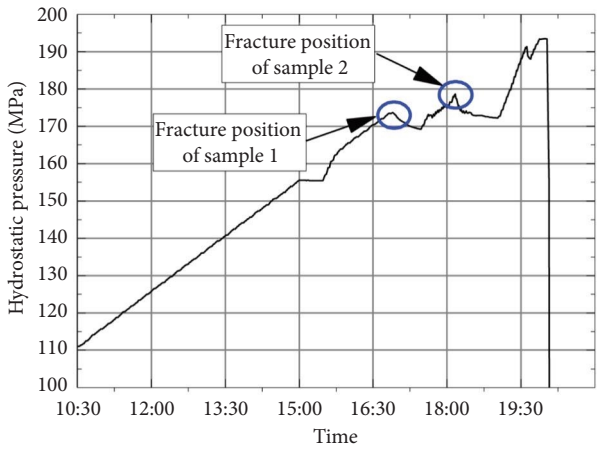

Figure 6: Ultimate strength test curve of *T*-68.

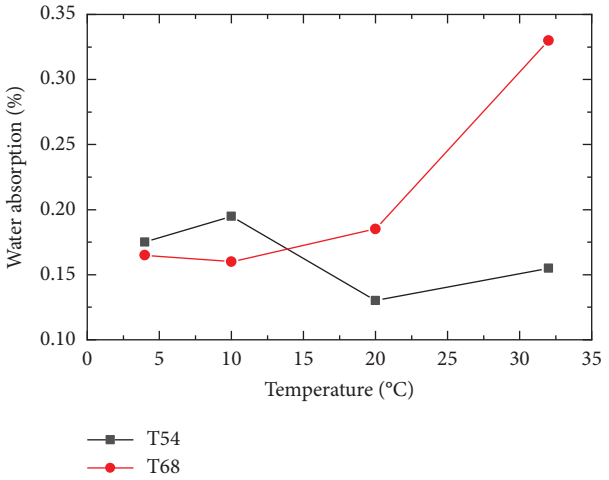

Figure 7: Water absorption vs. temperature.

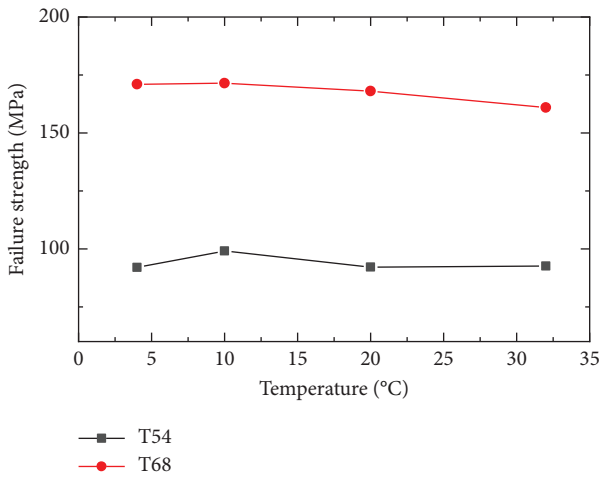

Figure 8: Failure strength vs. temperature.

working pressure at the rate of 25 MPa/min and maintained for 5 min. Afterward, the pressure was released. According to this procedure, it was loaded 100, 200, 400, 500, 600, and 800 times, and the water absorption and crushing strength of the material were measured, respectively, after 1000 times. Figure 11 shows the cyclic loading curve (five cycles).

Figures 12 and 13 show that the water absorption characteristics of the two buoyant materials increase exponentially as the number of cyclic loading increases, and the growth trend is similar. Considering the actual operating load spectrum of manned submersible, the maximum cyclic loading durations of buoyant materials is 1000 times. At this time, the water absorption values of T-54 and T-68 are 0.62% and 0.84%, respectively. The corresponding water absorption increases exponentially with the number of cycles, and the crushing strength of the two buoyant materials decreases linearly as the number of cycles increases. When the number of cycles is 800, the crushing strength characteristics of T-54 and T-68 decrease to 78 and 162 MPa, respectively. When the number of cycles is 1000, the crushing strength of T-54 decreases to 72 MPa, and its decrement rate is 23.4%. In contrast, the crushing strength of T-68 decreases to 160 MPa, and its decrement rate is 9.1%.

3.5. Failure Mode Analysis. Figure 14 shows the sample after the isostatic pressure loading failure. After the isostatic pressure failure test, the buoyant material sample is complete as a whole, and there are filamentous cracks, surface collapse,

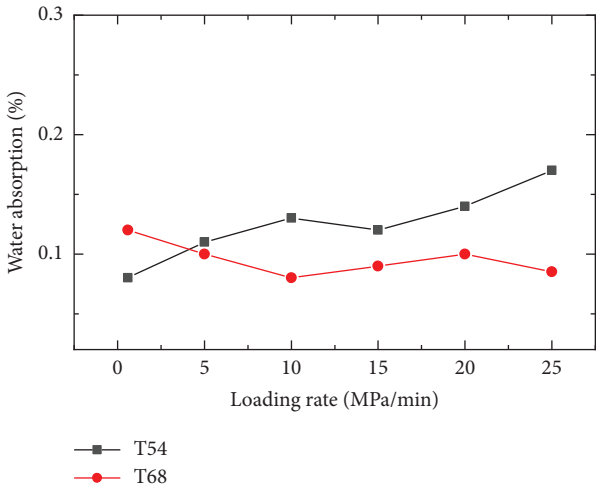

Figure 9: Water absorption vs. loading rate.

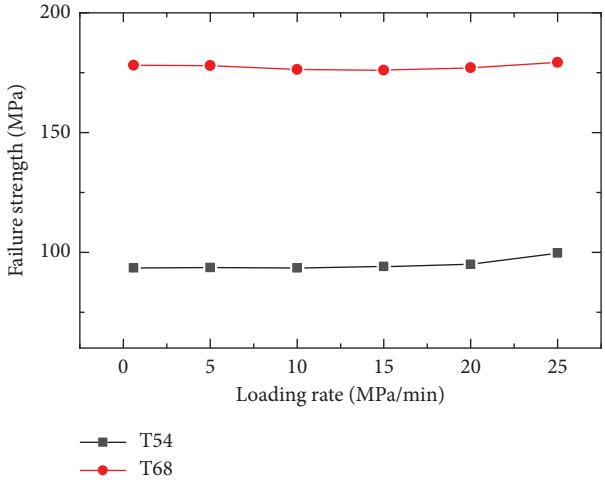

Figure 10: Failure strength vs. loading rate.

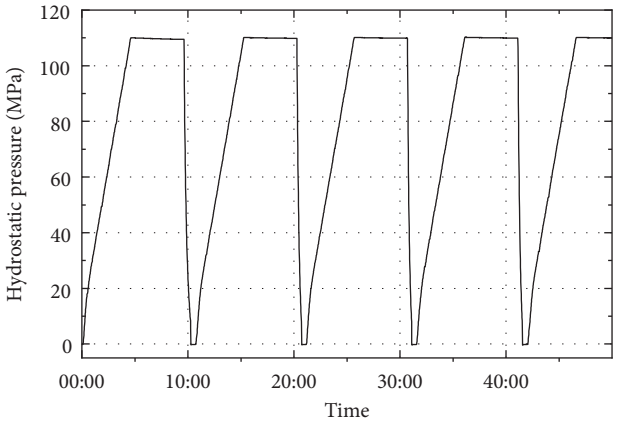

Figure 11: Cyclic loading curve (five cycles).

and even cracking on the sample surface. The failure mode of T-68 is filamentous cracks and local compression deformation. T-54 is mainly damaged in the form of middle

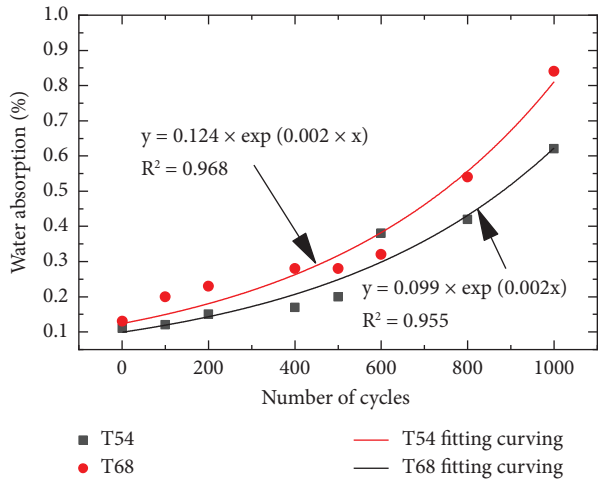

Figure 12: Water absorption vs. number of cycles.

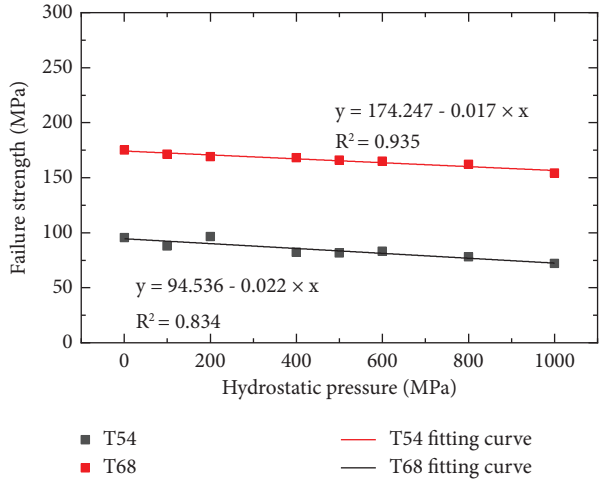

Figure 13: Failure strength vs. hydrostatic pressure.

expansion and compression at both ends, and individual samples form failure cracks at both ends.

3.6. Micromorphologies of Buoyant Materials. The micromorphologies and microstructures of buoyant materials can be observed directly by scanning electron microscope. Figure 15(a) shows that at 500 times magnification, the buoyancy material is composed of high-strength glass hollow microspheres and densely packed high-strength resin substrate. The diameters of the hollow microspheres differ, and the fracture edge can be clearly distinguished in the material crushing area. Figure 15(b) shows that the thickness of the edge of hollow microspheres is 1 μm.

X-ray micro-CT was used to analyze the micromorphology of the samples before/after cyclic loading, and Figure 16 shows that the data with the size of 600 μm × 600 μm × 600 μm were captured from the CT scanning data. Further quantitative analysis showed that the breakage rate of hollow glass beads inside the material did not change significantly before/after cyclic loading, and the breakage rate of the beads was low. It can be seen

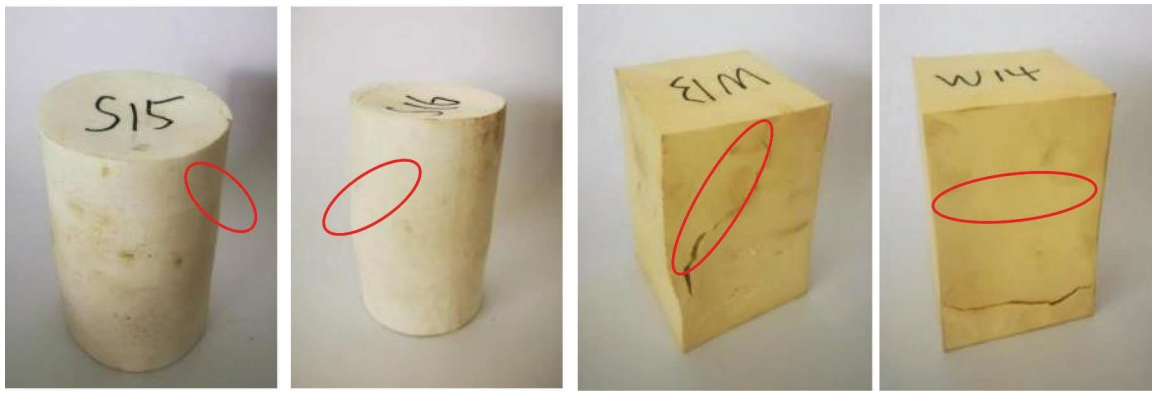

Figure 14: Sample picture after loading failure.

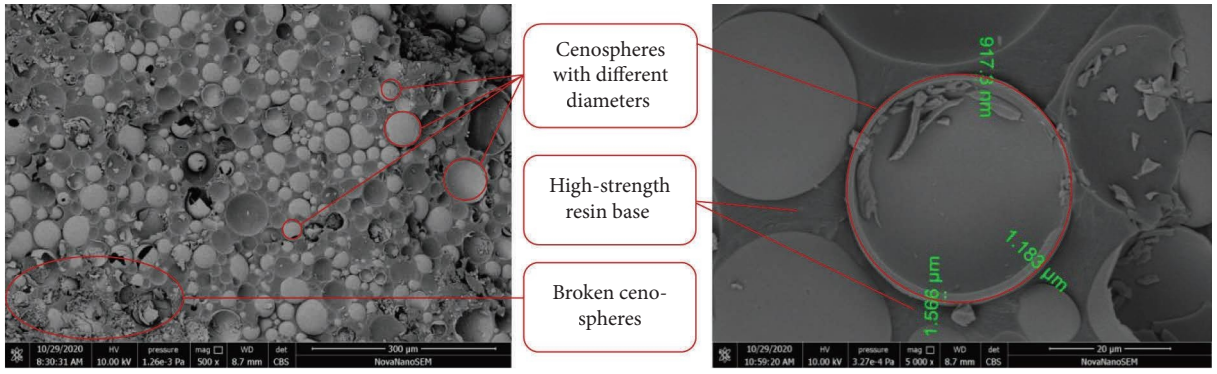

(a) 500 times (b) 5000 times

Figure 15: SEM image of buoyant material. (a) 500 times. (b) 5000 times.

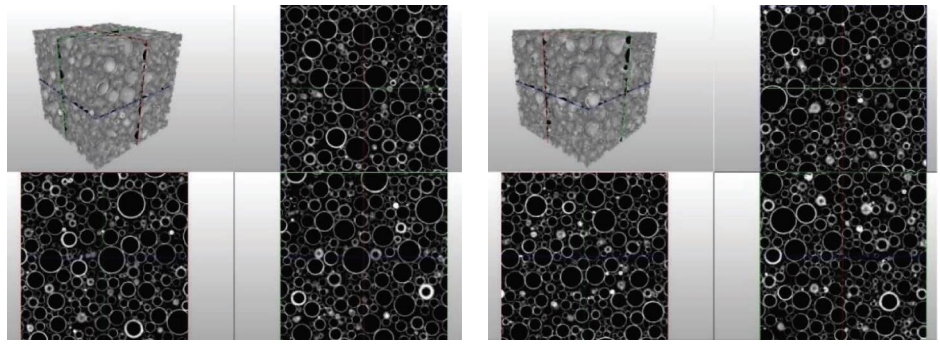

(a) (b)

Figure 16: Four views of local data. (a) Before cyclic loading. (b) After cyclic loading.

that the compressive resistance of hollow glass beads inside solid buoyant materials is better, and the change of material properties is mainly due to the change of resin base material properties, which leads to material aging and performance attenuation. The results show that the overall mechanical behavior of buoyant materials is strongly affected by the properties of the matrix [32]. For the long-term cyclic load test, the characteristics of the epoxy resin matrix of buoyant materials should be further studied.

3.7. Safety Analysis of Solid Buoyancy Materials. The tests helped determine that the performance of solid buoyancy materials shows an attenuation trend after long-term aging. There is no evaluation criterion for the effective service life of solid buoyancy materials in the relevant literature. With the long-term service of submersibles, the water absorption of solid buoyancy materials increases, and the crushing strength decreases, reducing the service safety factor. The water absorption causes the hydrolysis and swelling of epoxy resin, which reduces the bonding strength of hollow glass

beads and epoxy resin. Then, the compressive strength of solid buoyancy material is reduced, which endangers the safety of manned submersibles [33, 34]. According to the CCS specification for the water level of diving systems and submersibles, the safety factors of the water absorption characteristics of 1000- and 4500 m buoyant materials are 1.231 and 1.15, respectively. The safety factor of the crushing strength is 1.5. According to the cyclic test results, the crushing strength characteristics of the two buoyant materials decrease linearly as the number of cycles increases. T-54 has a greater safety factor; the number of cycles is 1000, and its crushing strength decreases to 72 MPa, still satisfying the specification requirements. Concerning T-68, the number of cycles is 800, its crushing strength decreases to 162 MPa, and the safety factor of the crushing strength is <1.5, which does not meet the specification requirements, so the buoyant material shall be inspected and replaced. After 1000 cycles, the water absorption of the two buoyant materials is <1%, still satisfying the specification requirements.

The water absorption of solid buoyancy materials decreases after long-term corrosion, which reduces the safety factor. Also, the buoyancy loss of buoyant materials increases due to the reduction in the performance of buoyant materials. The buoyancy loss of the buoyant material includes the buoyancy losses due to the increase in water absorption and the volume shrinkage. The volume shrinkage of buoyant materials under high hydrostatic pressure is independent of the shape and volume of buoyant material components but related to the uniformly distributed hydrostatic pressure and bulk elastic modulus. The volume shrinkage of buoyant materials is calculated as follows:

$$e = -\frac{p}{k}, \tag{3}$$

$$k = \frac{E}{3(1-2\mu)}, \tag{4}$$

where E is the Young's modulus of elasticity, and μ is Poisson's ratio, k is the bulk elastic modulus of the solid buoyancy materials, p is the hydrostatic pressure, e is the volume shrinkage of buoyant materials.

The buoyancy loss is calculated as follows:

$$F_1 = v_0 \times \rho \times \eta \times g, \tag{5}$$

$$F_2 = \Delta v \cdot \rho' \cdot g = v_0 \cdot e \cdot \rho' \cdot g, \tag{6}$$

where v_0 is the volume of solid buoyancy materials for manned submersibles, ρ is the density of solid buoyant materials, η is the water absorption of solid buoyancy materials, and ρ' is the density of seawater at the operating depth of the manned submersible. F_1 is the buoyancy losses due to the increase in water absorption, and F_2 is the buoyancy losses due to the volume shrinkage of buoyant materials. The sum of F_1 and F_2 represents the total buoyancy loss.

Figure 17 shows the curves of cyclic loading times against the buoyancy loss of "Shenhaiyonshi" manned submersibles and "Fendouzhe" manned submersibles at the design working depth calculated according to the test results. As the cyclic loading time increases, the water absorption characteristics of the buoyant materials decrease, and the buoyancy loss increases. For the "Fendouzhe" manned submersible with T-68, after 1000 loading cycles, the buoyancy loss value caused by the increase in water absorption of buoyant materials is close to the load of the manned submersible. Thus, the sampling test of water absorption of buoyant materials should be conducted regularly, which provides a basis for the counterweight calculation of manned submersible.

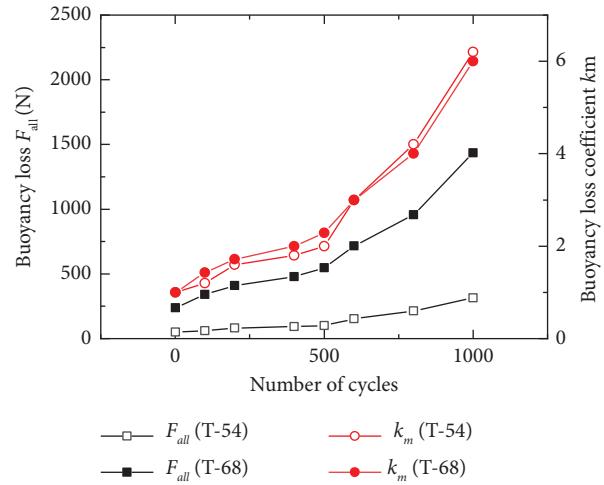

Figure 17: Cyclic load times vs. buoyancy loss.

4. Conclusion

To explore the influence mechanism of different pressure, temperature, loading rate, and load cycle times on deformation, failure, and water absorption behavior of solid buoyant materials, hydrostatic pressure tests of solid buoyant materials under different conditions are conducted in this study. Based on the test data, the nonlinear characteristics of mechanical properties and water absorption behavior of two buoyant materials are obtained. There are two major limitations in this study that could be addressed in future research. First, the findings of this study must be considered in the context of experimental limitations, the results were obtained in a freshwater environment, and the effect of seawater should be further considered for long-term cycling tests. The second limitation concerns the coupling parameters, limited by the test conditions; this study considers single conditions such as pressure strength, temperature environment, loading speed, and cycle times, respectively, and lacks multiparameter test coupling analysis. Nevertheless, the results we obtain are beneficial. The research results are summarized as follows:

(1) The water absorption characteristics of T-54 and T-68 are obviously affected by the hydrostatic pressure, and the changing trend is the same. When the hydrostatic pressure exceeds 80 MPa, the water absorption of T-54 increases exponentially. When

the hydrostatic pressure exceeds 100 MPa, the water absorption of T-68 increases exponentially. The loading rate has no obvious effect on the compressive strength and water absorption characteristics of the two materials.

(2) T-54 and T-68 are affected by the ambient temperature. When the ambient temperature exceeds 20°C, the water absorption of T-68 increases significantly, and the crushing strength decreases. In contrast, the water absorption and crushing strength of T-54 are unaffected significantly by the ambient temperature.

(3) After cyclic loading, the properties of buoyant materials decrease. As the cyclic loading time increases, the water absorption characteristics of the two materials increase exponentially, and the crushing strength decreases linearly as the cyclic loading time increase. When the number of cycles reaches 1000, the crushing strength of T-54 decreases to 72 MPa, and the decrement rate of the crushing strength is 23.4%. At this time, the crushing strength still satisfies the specification requirements. The number of cycles is 800, the crushing strength of *T*-68 decreases to 162 MPa, and the decrement rate of the crushing strength is 7.4%. At this time, the crushing strength safety factor is <1.5, which does not meet the specification requirements; thus, sampling inspection and replacement of buoyancy materials shall be conducted. After 1000 cycles of loading, the water absorption of the two materials is <1%, X-ray micro-CT showed that the internal hollow glass beads had a good shape and no significant change in glass beads breakage rate. The change of solid buoyancy material properties is mainly due to the change of resin base material properties, resulting in material aging and performance attenuation.

(4) With the long-term service of the submersible, the water absorption performance and buoyancy loss of the buoyant material decreases and increases, respectively. For the "Fendouzhe" manned submersible with *T*-68, after 1000 cycles of loading, the buoyancy loss caused due to the reduction of the water absorption of the buoyant material is close to the load of the manned submersible.

The outcomes of this study are helpful for us to understand the evolution law of buoyancy material properties, the influence law of temperature and temperature change on performance attenuation, the influence of loading strength and loading change mode on performance evolution, and the relationship between the setting of safety factor and service life of buoyancy materials, which are helpful for solving key problems such as accurate early warning and service life assessment of buoyancy materials. It provides the basis for realizing the health management in the whole life cycle of materials. In addition, the research results provide a basis for the calculation of counterweight in manned submersibles operation, the maintenance of manned submersibles, and the performance evaluation of manned submersibles in service under complex thermal and mechanical environment.

Data Availability

The data used during the study are obtained by the first author through experiments.

Conflicts of Interest

The authors declare that they have no conflicts of interest.

Authors' Contributions

Investigation, Writing—Original Draft Preparation, Visualization, Software, Resources, Project Administration, and Funding Acquisition, H. Z.; Investigation, Data Curation, and Formal Analysis, Z. Z. and G. M.

Acknowledgments

This work is financially supported by the Hainan Province Basic and Applied Basic Research Program (Natural Science) High-Level Talents Project of China (2019RC262).

References

[1] Q. Du, Y. Hu, and W. Cui, "Safety assessment of the acrylic conical frustum viewport structure for a deep-sea manned submersible," *Ships and Offshore Structures*, vol. 12, no. 1, pp. S221–S229, 2017.

[2] W. Cui, "Development of the Jiaolong deep manned submersible," *Marine Technology Society Journal*, vol. 47, no. 3, pp. 37–54, 2013.

[3] W. Cui, J. Guo, and B. B. Pan, "A preliminary study on the buoyancy materials for the use in full ocean depth manned submersibles," *Journal of Ship Mechanics*, vol. 22, pp. S736–S757, 2017.

[4] Z. Zhang, G. Liang, Q. Niu et al., "A wiener degradation process with drift-based approach of determining target reliability index of concrete structures," *Quality and Reliability Engineering International*, vol. 38, no. 7, pp. 3710–3725, 2022.

[5] C. Swetha and R. Kumar, "Quasi-static uni-axial compression behaviour of hollow glass microspheres/epoxy based syntactic foams," *Materials & Design*, vol. 32, no. 8-9, pp. 4152–4163, 2011.

[6] K. Ambika Devi, B. John, C. P. Reghunadhan Nair, and K. N. Ninan, "Syntactic foam composites of epoxy-allyl phenol-bismaleimide ternary blend-processing and properties," *Journal of Applied Polymer Science*, vol. 105, no. 6, pp. 3715–3722, 2007.

[7] M. Le Gall, D. Choqueuse, P. Y. Le Gac, P. Davies, and D. Perreux, "Novel mechanical characterization method for deep sea buoyancy material under hydrostatic pressure," *Polymer Testing*, vol. 39, pp. 36–44, 2014.

[8] X. Li, "Properties of deep-water solid buoyancy material," *Appl Eng Plast*, vol. 47, pp. 19–23, 2019.

[9] S. Yu, "Study on curing kinetics and properties of AFG-90 based solid buoyancy," *Transactions of Beijing Institute of Technology*, vol. 38, pp. 1205–1210, 2018.

[10] L. Li, L. Yu, C. Li, H. Zhao, and J. Yu, "Solid buoyancy material and research status on its properties," *Materials Review*, vol. 26, pp. 66–69, 2012.

[11] J. Wang, W. Chen, F. Wang et al., "Nutrition therapy for mitochondrial neurogastrointestinal encephalopathy with homozygous mutation of the TYMP gene," *Clinical nutrition research*, vol. 4, no. 2, pp. 132–136, 2015.

[12] S. Ren, A. Guo, X. Dong et al., "Preparation and characteristic of a temperature resistance buoyancy material through a gelcasting process," *Chemical Engineering Journal*, vol. 288, pp. 59–69, 2016.

[13] B. Jiang, G. Blugan, P. N. Sturzenegger et al., "Ceramic spheres-A novel solution to Deep Sea buoyancy modules," *Materials*, vol. 9, no. 7, p. 529, 2016.

[14] L. Chen, F. Wang, and W. Cui, "Effective elastic modulus characteristics of buoyancy materials of full-ocean-depth manned submersible," *Ship Mech*, vol. 23, pp. 1486–1499, 2019.

[15] A. Ali, C. Zhang, T. Bibi et al., "Investigation of five different low-cost locally available isolation layer materials used in sliding base isolation systems," *Soil Dynamics and Earthquake Engineering*, vol. 154, Article ID 107127, 2022.

[16] X. Liang, "Research on mechanical properties of syntactic foam under hydrostatic pressure circumstance," *Aging Appl Synth Mater*, vol. 49, pp. 5–7+4, 2020.

[17] L. Li, C. Su, L. Fan, F. Gao, X. Liang, and C. Gong, "Clinical and molecular spectrum of 46,XY disorders of sex development that harbour MAMLD1 variations: case series and review of literature," *Orphanet Journal of Rare Diseases*, vol. 15, no. 1, pp. 188–190, 2020.

[18] X. Liang, J. Gao, D. Li, and X. Cao, "Cloning and expressions of peroxisome proliferator activated receptor alpha1 and alpha2 (PPARα1 and PPARα2) in loach (*Misgurnus anguillicaudatus*) and in response to different dietary fatty acids," *Biochemical and Biophysical Research Communications*, vol. 481, no. 1-2, pp. 38–45, 2016.

[19] N. Gupta and E. Woldesenbet, "Compressive fracture features of syntactic foams-microscopic examination," *Journal of Materials Science*, vol. 37, no. 15, pp. 3199–3209, 2002.

[20] J. Z. Liang, "Tensile and impact properties of hollow glass bead-filled PVC composites," *Macromolecular Materials and Engineering*, vol. 287, no. 9, pp. 588–591, 2002.

[21] J. Z. Liang, "Mechanical properties of hollow glass bead-filled ABS composites," *Journal of Thermoplastic Composite Materials*, vol. 18, no. 5, pp. 407–416, 2005.

[22] J. Z. Liang, "Impact fracture toughness of hollow glass bead-filled polypropylene composites," *Journal of Materials Science*, vol. 42, no. 3, pp. 841–846, 2007.

[23] K. Q. Yan, H. Xie, and J. J. Zhang, "Research on mechanical properties of high-performance hollow glass microspheres," *Materials Reports*, vol. 25, no. 9, pp. 116–130, 2011.

[24] N. Gupta and E. Woldesenbet, "Microballoon wall thickness effects on properties of syntactic foams," *Journal of Cellular Plastics*, vol. 40, no. 6, pp. 461–480, 2004.

[25] H. S. Kim and P. Plubrai, "Manufacturing and failure mechanisms of syntactic foam under compression," *Composites Part A: Applied Science and Manufacturing*, vol. 35, no. 9, pp. 1009–1015, 2004.

[26] S. Bo, W. Chen, and D. J. Frew, "Dynamic compressive response and failure behavior of an epoxy syntactic foam," *Journal of Composite Materials*, vol. 38, no. 11, pp. 915–936, 2004.

[27] U. E. Ozturk and G. Anlas, "Hydrostatic compression of anisotropic low density polymeric foams under multiple loadings and unloadings," *Polymer Testing*, vol. 30, no. 7, pp. 737–742, 2011.

[28] Q. Zhao, "Research on damage mechanism of buoyancy materials for deep sea manned submersibles," *Huazhong Univ of ci & Tech*, vol. 48, pp. 104–108, 2020.

[29] J. Wang, W. Cui, and A. Water, "Absorption model based on self- consistent theory for solid buoyancy materials," *Engineering and Technology*, vol. 3, pp. 00119–00129, 2020.

[30] S. L. Pan, J. J. Zhang, and G. Z. Song, "Research progress of hollow glass microsphere and solid buoyant material fo deep-sea application," *Journal of Tropical Oceanography*, vol. 28, no. 4, pp. 17–21, 2009.

[31] Z. Zhang, F. Yang, H. Zhang et al., "Influence of CeO2 addition on forming quality and microstructure of TiC -reinforced CrTi4-based laser cladding composite coating," *Materials Characterization*, vol. 171, Article ID 110732, 2021.

[32] J. R. M. d'Almeida and S. N. Monteiro, "The resin/hardener ratio as a processing parameter for modifying the mechanical behaviour of epoxy-matrix/glass microsphere composites," *Composites Science and Technology*, vol. 58, no. 10, pp. 1593–1598, 1998.

[33] B. Lana, "Influence of hydrolysis on properties of organicinorganic hybrid materials based on epoxy resin," *Hrvatska znanstvena bibliografija i MZOS-Svibor*, 2009.

[34] Y. Wang, H. Wang, B. Zhou, and H. Fu, "Multi-dimensional prediction method based on Bi-LSTMC for ship roll," *Ocean Engineering*, vol. 242, Article ID 110106, 2021.